European Journal of Medicinal Chemistry 135 (2017) 77–88

Contents lists available at ScienceDirect

European Journal of Medicinal Chemistry

journal homepage: http://www.elsevier.com/locate/ejmech

Research paper

Novel lipid-mimetic prodrugs delivering active compounds to adipose tissue

Andrea Mattarei [a, **, 1], Andrea Rossa [a, b, c], Veronica Bombardelli [a, b, c], Michele Azzolini [b, c], Martina La Spina [c], Cristina Paradisi [a], Mario Zoratti [b, c], Lucia Biasutto [b, c, *]

[a] University of Padova, Department of Chemical Sciences, Via F. Marzolo 1, 35131 Padova, Italy
[b] CNR Neuroscience Institute, Viale G. Colombo 3, 35121 Padova, Italy
[c] University of Padova, Department of Biomedical Sciences, Viale G. Colombo 3, 35121 Padova, Italy

ARTICLE INFO

Article history:
Received 30 January 2017
Received in revised form
20 March 2017
Accepted 11 April 2017
Available online 13 April 2017

Keywords:
Pterostilbene
Triglyceride
Lipid-mimetics
Adipose tissue targeting

ABSTRACT

Obesity and associated pathologies are a dramatically growing problem. New therapies to prevent and/or cure them are strongly needed. Adipose tissue is a logical target for pharmacological intervention, since it is now recognized to exert an important endocrine function, secreting a variety of adipokines affecting, for example, adiposity and insulin resistance. This proof of principle work focuses on the development of novel lipid-mimetic prodrugs reaching fat deposits by the same lymphatic absorption route followed by dietary triglycerides.

Pterostilbene, a natural phenolic compound with potential anti-obesity effects, was used as model "cargo", attached via a carbamate group to an ω-aminodecanoate chain linked to either position 1 or position 2 of the glycerol moiety of synthetic triglycerides. The prodrugs underwent position-selective hydrolysis when challenged with pancreatic lipases *in vitro*. Pterostilbene-containing triglycerides as well as pterostilbene and its metabolites were present in the adipose tissue of mice fed an obesogenic diet containing one or the other of the derivatives.

For the first time this approach is used to deliver an obesity antagonist to the adipose tissue. The results demonstrate the feasibility of delivering active compounds to adipose tissue by reversibly incorporating them into triglyceride-mimetic structures. Upon release in the target site these compounds are expected to exert their pharmacological activity precisely where needed.

1. Introduction

Obesity has been firmly correlated with an increased hazard for a range of serious ailments [1,2]. The strongest link [3] may be that between the overweight/obese status and the metabolic syndrome, defined as "a compilation of risk factors that predispose individuals to the development of type 2 diabetes (T2D) and cardiovascular disease (CVD)" [4]. White adipose tissue (WAT) secretes adipokines (leptin, adiponectin and several others) which have major (patho) physiological effects and mediate interactions between WAT and other organs, including the immune system, liver, muscle and the central nervous system [5]. For example, adiponectin levels decrease in adiposity, contributing to obesity-associated cancerogenesis, CVD and T2D.

Upward violation of adipose tissue homeostasis leads to the immigration of macrophages and to an increase of pro-inflammatory cytokines such as TNFα, IL-1β, IL-6, as well as of iNOS and ROS, which can act in paracrine/endocrine fashion leading to a chronic inflamed state linked to a host of pathologies [6]. Systemic oxidative stress [7] contributes heavily itself to the onset and progression of obesity-associated health problems [8]. Thus, developing effective tools against adiposity on one hand and its consequences on the other are strong priorities of modern pharmacology. The most successful treatment for obesity is an appropriate reduction of food intake, accompanied by exercise [9]. Exercise seems also to ameliorate the inflammatory status, independently from weight loss [10], and to induce "browning" of white

* Corresponding author. CNR Neuroscience Institute c/o Dept. of Biomedical Sciences, Viale G. Colombo 3, 35121 Padova, Italy.
** Corresponding author.
E-mail addresses: andrea.mattarei@unipd.it (A. Mattarei), lucia.biasutto@cnr.it (L. Biasutto).
[1] Present address: Department of Pharmaceutical & Pharmacological Sciences, University of Padova, Via F. Marzolo 5, 35131 Padova, Italy.

http://dx.doi.org/10.1016/j.ejmech.2017.04.034
0223-5234/

fat [11,12]. Brown fat (BAT) [11,13,14] is a mitochondria-rich type of adipose tissue, abundant in early life, which provides - normally when prompted by the sympathetic nervous system - non-shivering thermogenesis, dissipating food-derived energy to produce heat in mitochondria "uncoupled" by the expression of Uncoupling Protein 1 (UCP1). It can thus counteract obesity. An important role in the complex regulation of BAT is attributed to AMPK, expressed both in the controlling CNS structures and in adipose tissue: reduction of AMPK activity in the hypothalamus or upregulation of it in WAT and BAT increase "browning" and energy dissipation [15]. AMPK signaling, activated by exercise, has to do with insulin secretion, glucose transport, mitochondrial biogenesis, fatty acid oxidation, inflammation. Development of anti-obesity drugs has registered some failures, due to important side effects, and has so far not had a significant impact on population-wide obesity [16]. A few drugs are currently available which have shown some modest efficacy and side effects ranging from constipation to tumorigenesis (in experimental animals) [17]. They are costly, some are classified as controlled substances because of the possibility of abuse, all are off-limits in pregnancy and lactation. The possibility of BAT recruitment by pharmacological intervention is receiving much attention [13,18]. Organ-specific upregulation of AMPK activity may provide a strategy (see above). Indeed metformin, an AMPK activator and a major anti-diabetic drug, also induces weight loss [19].

Natural compounds may arguably be considered the best currently available weapons in the anti-obesity, anti-metabolic disorder arsenal [20–22]. For example berberine, genistein, flavonoids, catechins and resveratrol indirectly activate AMPK [23]. Resveratrol [24–26] is just the most talked-about member of the family of bioactive stilbene polyphenols, whose mechanisms of action are thought to overlap to a considerable degree [27]. Upregulation of UCP1 by resveratrol may account for the energy dissipation that must take place for a "slimming" effect [28]. Its efficacy is limited however by its prompt and extensive modification by Phase II metabolism enzymes, for which it represents a ready-made target [29]. Pterostilbene, i.e. 3,5-di-O-methylresveratrol [30–32], having only one free hydroxyl, is less prone to metabolic conjugation, has a relatively high bioavailability [33,34] and a potentially higher efficacy than resveratrol [35,36]. Of relevance, the prodrug approach to increasing absorption and reducing metabolic conjugation and elimination offers more promise with pterostilbene than with resveratrol, due to the need to protect only one hydroxyl instead of three [37].

The ability of pterostilbene to antagonize the metabolic syndrome has been reported by several studies [38–40]. Like resveratrol, it can activate the Keap/Nrf2/ARE anti-oxidant pathway, upregulate SIRT1, repress NF-kB activity, activate AMPK. It has been reported to upregulate adiponectin in an *in vitro* 3T3-L1 adipocyte cell model [41] and to downregulate instead the secretion of pro-inflammatory cytokines upon interaction of these cells with RAW 264.7 macrophages [42].

It is clear that a strategy for the selective pharmacological targeting of adipose tissue would represent a powerful tool in the fight against obesity and obesity-related problems. As discussed, the issue is not just that of reducing fat deposits, but also that of relieving chronic inflammation where needed.

Based on these premises, this work is focused on the development of a tool to selectively convey a representative active phenolic compound (APC), pterostilbene, to adipose tissue by imitating intestinal lipid absorption [43]. In the intestinal lumen dietary triglycerides are degraded by pancreatic lipases (PL), which hydrolyze the ester bonds selectively at position 1 in the glycerol backbone. Free fatty acids and monoglycerides pass then into enterocytes, where triglycerides are resynthesized and packed into chylomicrons. These are preferentially taken up into the lacteals of the lymphatic system rather than into the portal vein - thus avoiding first-pass metabolism - and eventually move to the thoracic duct and into the blood. Plasma triglyceride levels are regulated by the lipoprotein lipase (LPL) system [44], which hydrolyzes triglycerides to fatty acids for concomitant use or storage by the underlying tissue.

As a proof of principle study, we have thus undertaken the synthesis of lipid-mimetic prodrugs of pterostilbene to exploit the efficient and selective distribution of triglycerides, through the lymphatic system, to adipose tissue (Fig. 1).

In our approach the APC is incorporated into a long-chain triglyceride. Two classes of isomeric derivatives can be synthesized and tested, characterized by connection of the APC either to position 1 (Type-1) or 2 (Type-2) of the glycerol backbone (Fig. 2).

A similar strategy has been adopted in a few previous studies [45–48]. To our knowledge, however, in no case the construct was meant to target the adipose tissue.

The prodrugs we synthesized underwent position-selective hydrolysis when challenged with Pancreatic Lipase *in vitro*. Pterostilbene-containing triglycerides as well as pterostilbene and its metabolites were present in the adipose tissue of mice fed an obesogenic diet containing one or the other of the derivatives. These results provide evidence that this approach can succeed in delivering a cargo to the adipose tissue after oral administration.

2. Results and discussion

2.1. Synthesis of lipid-mimetic prodrugs of pterostilbene

Pterostilbene was reversibly linked to the triglyceride structure through a carbamate bond. The choice was based on previous results, which showed that this group is resistant to hydrolysis by digestive enzymes in the stomach and intestine, but releases the active compound at convenient rates after passing into the blood and tissues [49,50]. The length of the linker chain (*n* in Fig. 2) has been chosen arbitrarily as nine methylene units but can be modulated to optimize the performance of the derivatives. Details of the syntheses are provided in Materials and Methods.

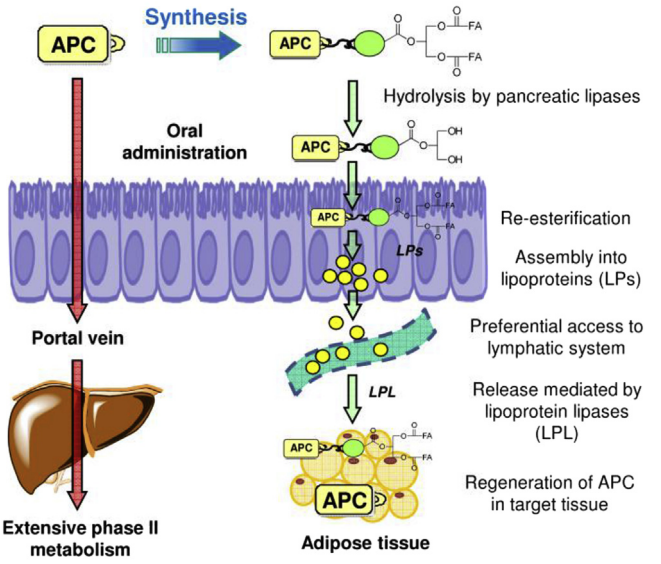

Fig. 1. Absorption mechanisms expected for an active phenolic compound (APC) and for its triglyceride-mimetic prodrug. Only the Type-2 derivative is depicted.

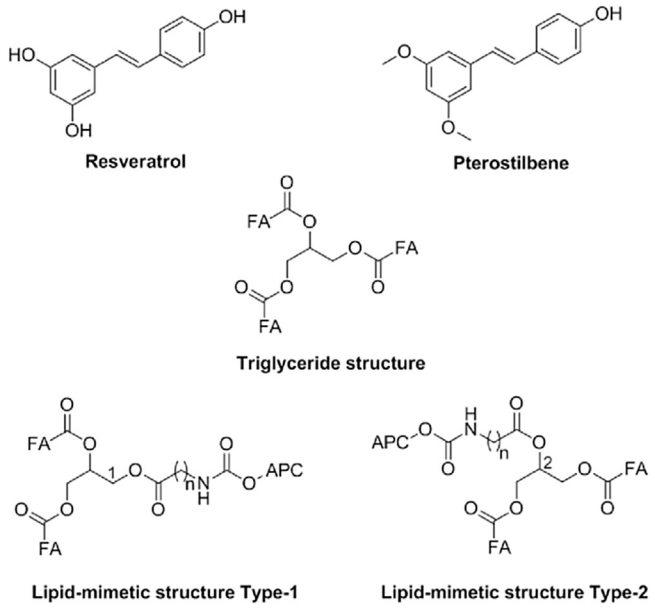

Fig. 2. Molecular structures of resveratrol, pterostilbene and lipid-mimetic prodrugs of active phenolic compounds.

2.2. Pancreatic lipase (PL) assays

Type-1 and Type-2 lipid-mimetic derivatives of pterostilbene were subjected to PL-catalyzed hydrolysis to verify whether the enzyme recognized them as "normal" triglycerides despite the presence of the cargo molecule.

Since PL catalyzes the hydrolysis of triglycerides ester bonds with a marked preference for the external positions (1 and 3 of the glycerol backbone), one would expect to observe as main hydrolysis processes those shown in Fig. 3. Type-1 is a chiral compound, but structural differences distinguishing substituents are distant from the chiral carbon (C-2) and the site of hydrolysis. It is therefore unlikely that the two enantiomers undergo hydrolysis at detectably different rates.

The kinetic results are reported in two graphs (Fig. 4) showing the variation in time of the amount of Type-1 (Fig. 4A) and Type-2 (Fig. 4B) derivatives and of their hydrolysis products, detected and quantified by HPLC/UV. In the chromatograms relative to the Type-1 derivative, as expected, only three species were visible: the Type-1 derivative itself, the product of partial hydrolysis **1**, and the carboxylic acid **2**. As shown in Fig. 4A, **2** formed at a rate comparable to that of the disappearance of Type-1. The only other near UV-absorbing molecule detected in the reaction solution, **1**, formed from the start and disappeared after reaching a maximum relative concentration of less than 5%. Fig. 4B shows the concentration profiles of four species: the Type-2 derivative, the products of partial hydrolysis **3** and **4**, and the carboxylic acid **2**. The formation of the latter in this case was slower than in the case of Type-1. Moreover, the high concentration reached by **4** and its relative stability under the reaction conditions is also consistent with the known preference of PL enzymes for attack at the external chains (positions 1 and 3 of the glycerol backbone), while the hydrolysis of the ester bond in position 2 is considerably slower.

The disappearance of the Type-1 prodrug is adequately fitted by an exponential decay; the derived rate constant k_1 ($3.24 \pm 0.09\ h^{-1}$, which is the sum of k_1' and k_1'', i.e. the two parallel hydrolysis processes shown in Fig. 3A) is very similar to that obtained for the Type-2 derivative ($3.04 \pm 0.07\ h^{-1}$; see below), and suggests that enzymatic hydrolysis at position 1 is not influenced by the presence

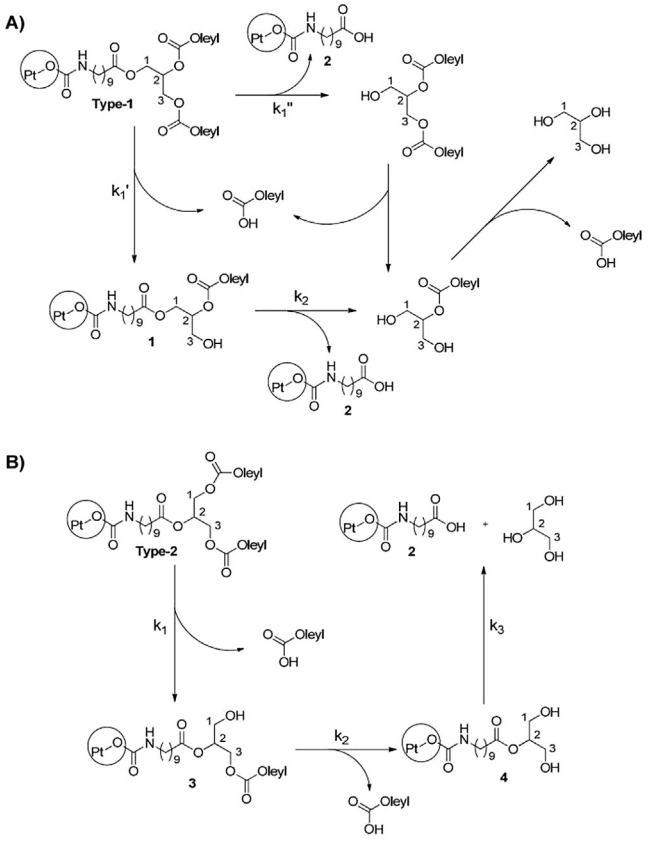

Fig. 3. Main hydrolysis process of Type-1 (panel A) and of Type-2 (panel B) derivatives in the presence of PL. Only the molecules containing pterostilbene in their structure are detectable by HPLC/UV (by their absorption, 300–320 nm).

of pterostilbene in the chain linked at that position. Since the levels of **1** are very low and its generation is regulated by k_1', we can hypothesize that its hydrolysis is very rapid. This hypothesis is supported by kinetic analysis of the appearance of **2**; fitting the data with a simple exponential equation ($y = 100 - y_0 \cdot e^{-kt}$) yields a kinetic constant ($2.88 \pm 0.07\ h^{-1}$) very similar to that describing the disappearance of the Type-1 derivative. The fitting of the experimental data is shown in Fig. 4A. In the case of the Type-2 prodrug, kinetic analysis of the data was performed by assuming that hydrolysis of the ester bonds occurs via consecutive losses of the three acyl chains in pseudo first-order processes (see Fig. 3B). The experimental data were fitted to estimate the hydrolysis rate constants (k_1, k_2, k_3) using the set of equations utilized by Mattarei et al. [51] for similar three-step hydrolysis processes. To simplify the kinetic analysis, the rate constants of hydrolysis at position 2 of Type-2 and **3** were considered to be negligible in comparison to k_1 and k_2. This assumption is justified *a posteriori* by the relative values calculated for k_1, k_2 and k_3 (Fig. 4B). The rate constants relative to the hydrolysis of the two external ester bonds (k_1 and k_2) have the same order of magnitude. k_2 is larger indicating that hydrolysis of the second ester bond in the external positions of the glycerol backbone is faster than hydrolysis of the first. According to the model, the rate constant for the hydrolysis of the central ester bond (k_3) is considerably lower: approximately 1/13 of k_1 and 1/40 of k_2 respectively.

In summary, the results of these experiments confirm that PL recognizes these lipid-mimetic prodrugs and handles them as if they were normal dietary lipids. Interestingly in neither case we were able to detect, even after 23 h of reaction time, the formation

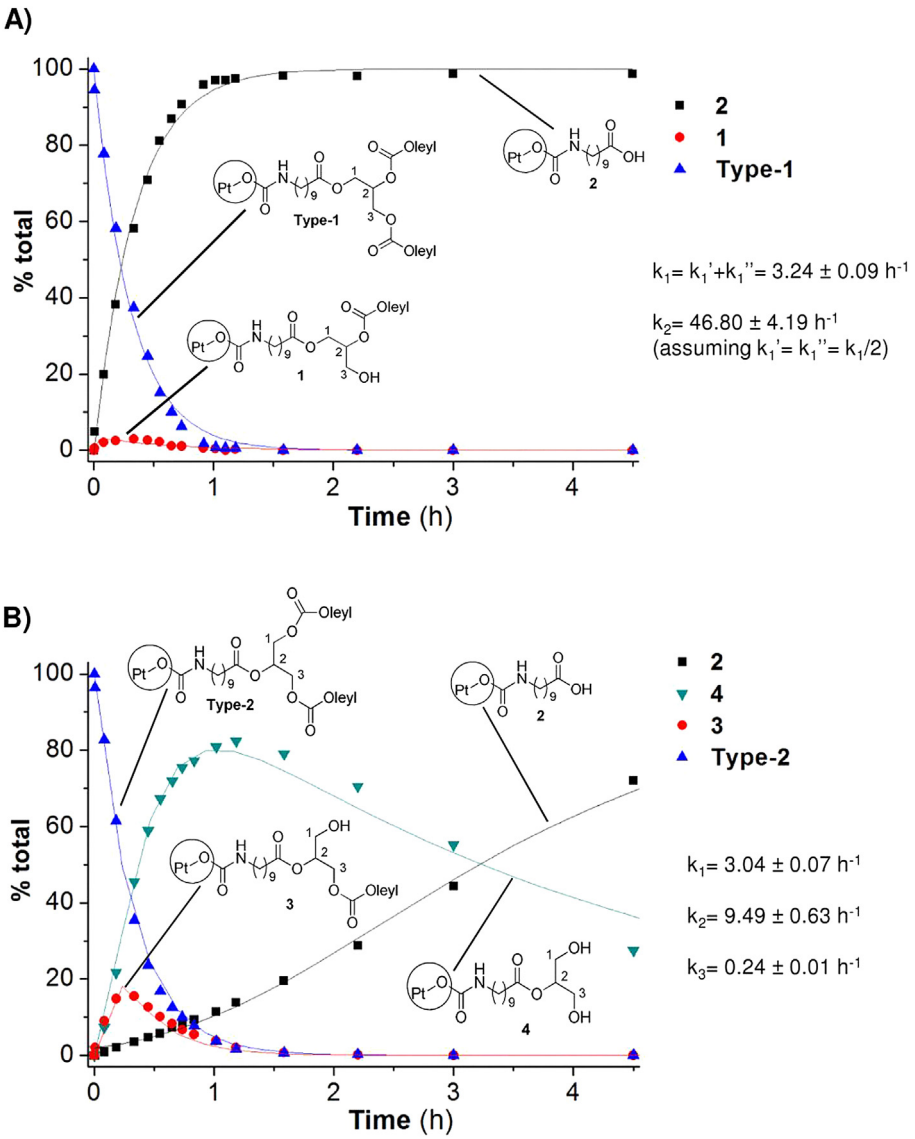

Fig. 4. Time-dependent relative abundance of Type-1 (panel A) and Type-2 (panel B) derivatives and UV-detectable species originated by their hydrolysis in the presence of PL.

of any pterostilbene, demonstrating the stability of the carbamate bond toward PL.

2.3. Tissue distribution

To assess if lipid mimetic derivatives actually reached the adipose tissue and regenerated pterostilbene *in vivo*, we performed tissue distribution experiments in mice, chronically administering the derivatives for 2 weeks in a high-fat diet regimen (see Materials and Methods for details).

Derivatives were found to reach in intact form the visceral and subcutaneous adipose tissue (Fig. 5A); while statistical significance was not reached, in both cases the levels of the Type-2 compound were higher than those of Type-1. Fig. 5B shows illustrative HPLC/UV (320 nm) chromatograms of the extract from the visceral adipose tissue of an animal chronically fed Type-2 derivative in high-fat chow (trace a), of the extract from adipose tissue from an untreated mouse (control) spiked with Type-2 derivative (trace b) and of an extract from control adipose tissue spiked with pterostilbene (trace c). Panel C shows an expanded view of the chromatogram region comprising the triglyceride peaks for two exemplary samples obtained from a mouse chronically fed Type-2 compound (trace a) and from a mouse chronically fed Type-1 compound (trace b). At least four non-background peaks are clearly present at retention times between 5.8 and 6.5 min in trace a (Type-2). In trace b (Type-1) the three peaks eluting at shorter retention times are barely, if at all, visible. Other minor HPLC peaks with an absorption spectrum typical of pterostilbene-containing species and eluting earlier than the triglycerides were also observed in most samples and can be attributed to partial hydrolysis products. The interpretation of the analytical data we propose is as follows: the partial hydrolysis by pancreatic lipases in the intestinal lumen and subsequent re-esterification into triglycerides in the enterocytes originates derivatives bearing fatty acid chains which may be different from those present in the administered derivative. This may account for the multiplicity of peaks observed in the triglyceride region. The major peak remains that corresponding to the administered prodrug, indicating that part of the latter actually reaches the adipose tissue in its original form. Interestingly, the peaks tentatively attributed to an exchange of the fatty acid chains

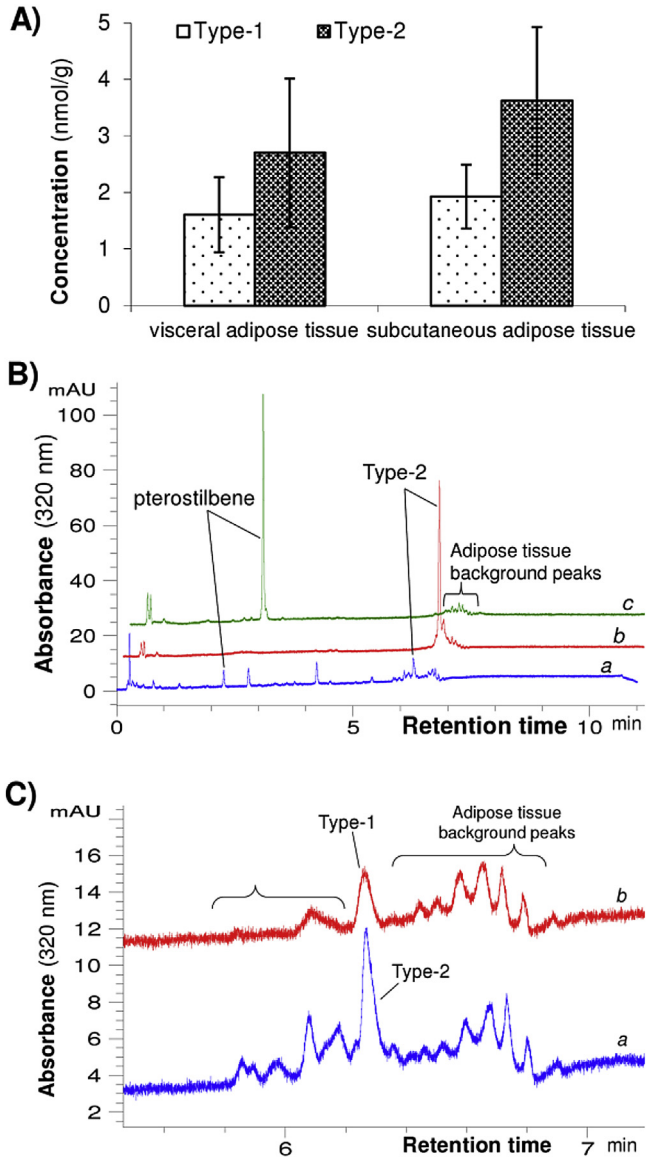

Fig. 5. A) Concentration of Type-1 and -2 derivatives in visceral and subcutaneous adipose tissue after a 2-week chronic treatment (see text for details). Mean values ± st. dev., N ≥ 4. B) HPLC/UV chromatograms (320 nm) of adipose tissue extracts from a mouse treated with Type-2 derivative for 2 weeks (trace a), or from an untreated animal, spiked with Type-2 derivative (trace b) or pterostilbene (trace c). C) Expanded segments of HPLC/UV chromatograms (320 nm) produced by extracts from the visceral adipose tissue of a mouse fed our Type-2 compound (trace a) and from the visceral adipose tissue of a mouse fed Type-1 compound (trace b). Shown is the region containing peaks attributed to triglycerides.

are much more evident in the case of Type-2 derivative: they may represent roughly as much pterostilbene as the intact prodrug itself. In this case the ester bond connecting the pterostilbene-containing chain to the glycerol backbone is resistant to lipase-mediated hydrolysis: pterostilbene therefore remains attached while the oleic acid linked to positions 1 and 3 is (in part) traded for other (endogenous) fatty acids; the resulting triglycerides reach the adipose tissue and can be detected thanks to the characteristic UV-absorption by the pterostilbene moiety. In the case of the Type-1 derivative pterostilbene is linked to position 1. It is therefore lost preferentially, and only in a minority of cases are the pterostilbene-containing chains "recycled" and joined to a glycerol backbone, eventually reaching the adipose tissue.

Taken together, the data support the hypothesis that lipid-mimetic derivatives are actually absorbed and handled *in vivo* as normal dietary triglycerides.

Finally, we carried out the determination of pterostilbene and of its main phase II metabolites, pterostilbene sulfate and glucuronide, in major organs of mice receiving either Type-1 or Type-2 triglyceride (Fig. 6A and B). Pterostilbene was present in the adipose tissues in both cases. Among the tissues analyzed, liver and adipose tissue turned out to have the highest levels of pterostilbene itself, while undetectable or very low concentrations of pterostilbene were found in the bloodstream (Fig. 6A and B).

To conclude, we have synthesized two variants of a triglyceride incorporating an obesity-antagonizing natural compound. These derivatives behave as expected for natural triglycerides in *in vitro* lipolysis assays and upon oral administration *in vivo*, reaching the adipose tissue with their "cargo". They may therefore represent a useful strategy to convey pharmacologically active molecules to this tissue.

2.4. Innovation

This study demonstrates for the first time that lipid-mimetic

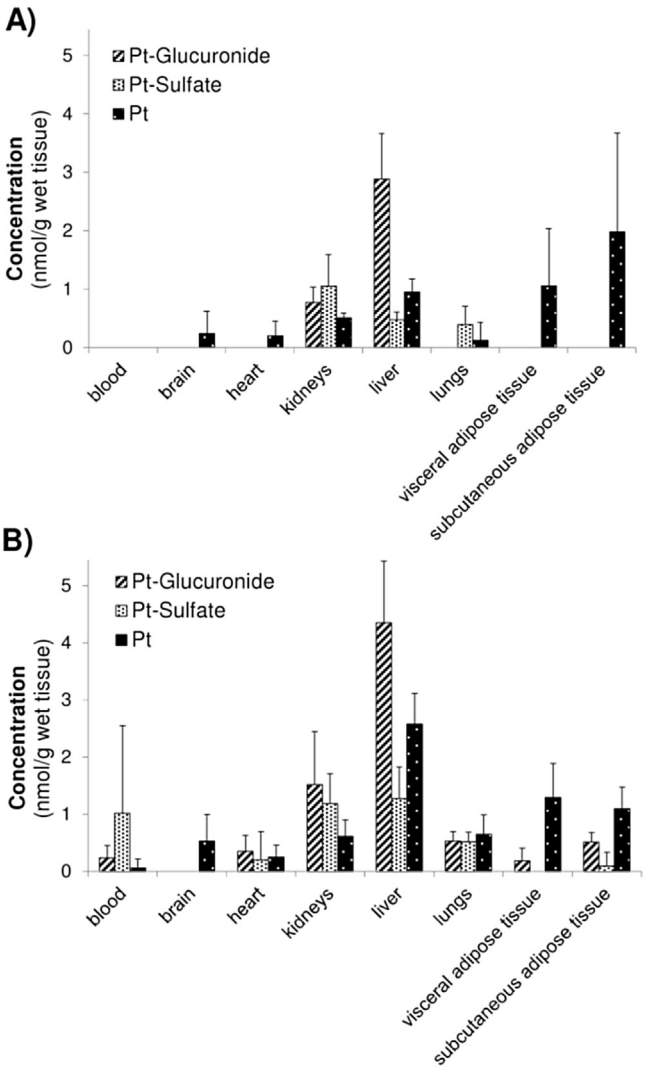

Fig. 6. Concentration of pterostilbene and metabolites in different organs of mice after a 2-week chronic administration of Type-1 (panel A) or Type-2 (panel B) derivatives (please see Materials and Methods for experimental details). Mean values ± st. dev., N ≥ 5.

derivatives are actually able to target the adipose tissue, and they are thus a useful strategy to convey pharmacologically active molecules to this tissue.

3. Materials and methods

3.1. Chemicals and instrumentation

Pterostilbene was obtained from Wonda Science (North Waltham, MA, USA, cat. n. 25992). Lindlar catalyst was obtained from Alfa Aesar (Karlsruhe, Germany, cat. n. 43172). Pterostilbene-4'-sulfate was synthesized as described in Azzolini et al. [34]. HPLC grade acetonitrile (MeCN) and THF were obtained from VWR and used without further purification. Other reagents and solvents were purchased from Sigma Aldrich (Milan, Italy), and were used as received: 1,10-decanediol (cat. n. D1203), periodic acid (cat. n. 375810), pyridinium chlorochromate (PCC; cat. n. 190144), oxalyl chloride (cat. n. O8801), oleoyl chloride (cat. n. 367850), sodium azide (cat. n. 199931), bis(4-nitrophenyl) carbonate (cat. n. 161691), 2,4,6-trimethylpyridine (cat. n. 27690), *p*-toluenesulfonic acid (PTSA; cat. n. 402885), 2,2-dimethoxypropane (cat. n. D136808), TRIS hydrochloride (cat. n. T3253), sodium periodate (cat. n. 363642), potassium phosphate monobasic (cat. n. P5655), pyridine (cat. n. 270970), triethylamine (TEA; cat. n. T0886), 4-(dimethylamino)pyridine (DMAP; cat. n. 107700), lithium aluminum hydride solution (1.0 M in THF, cat. n. 212776), lipase from porcine pancreas (Type VI-S, ≥20,000 units/mg protein, lyophilized powder, cat. n. L0382), colipase from porcine pancreas (essentially salt-free, lyophilized powder, cat. n. C3028). TLCs were run on silica gel supported on plastic (Macherey-Nagel Polygram®SIL G/UV254, silica thickness 0.2 mm) and visualized by UV detection or $KMnO_4$ oxidation. Flash chromatography was performed on silica gel (Macherey-Nagel 60, 230–400 mesh granulometry (0.063–0.040 mm)) under air pressure. Mass spectrometry analyses were performed with a 1100 Series Agilent Technologies system, equipped with binary pump (G1312A) and MSD SL Trap mass spectrometer (G2445D SL) with ESI source. ESI-MS positive and negative spectra of reaction intermediates and final purified products were obtained from solutions in methanol (MeOH) or MeCN, eluting with MeOH or MeCN containing 0.1% formic acid (only for positive mass spectra). ^{1}H and ^{13}C NMR spectra were recorded with a Bruker AV300 FT-NMR UltraShield operating at 300 MHz (for ^{1}H NMR) and 75 MHz (for ^{13}C NMR). Chemical shifts (δ) are given in parts per million (ppm) relative to the signal of the solvent. The following abbreviations are used to indicate multiplicities: s, singlet; d, doublet; dd, doublet of doublets; t, triplet; m, multiplet; br, broad signal.

3.2. Synthesis of (Z)-3-((10-(((4-((E)-3,5-dimethoxystyryl) phenoxy)carbonyl) amino)decanoyl)oxy) propane-1,2-diyl dioleate (Type-1 prodrug)

The synthesis of Type-1 lipid mimetic derivative of pterostilbene is outlined in Scheme 1. The first step in the synthesis was the esterification of a commercially available isopropylidene protected form of glycerol (**5**) with 10-chlorodecanoyl chloride (**SI-1**, see Supporting Information S3) to obtain the 1-ω-chloro substituted ester intermediate (**6**). After the cleavage of the acetonide-protecting group, the resulting glycol (**7**) was esterified using oleoyl chloride to obtain the 1-ω-chloro substituted triglyceride intermediate (**8**). This was treated with sodium azide in DMF to obtain the corresponding 1-ω-azide (**9**), which was then reduced using hydrogen in the presence of Lindlar catalyst and bis(4-nitrophenyl)carbonate to achieve the lipid mimetic 4-nitrophenyl activated urethane (**10**). This was finally transesterified with pterostilbene to obtain the desired lipid mimetic Type-1 derivative. The synthesis proceeds with good to excellent yields in isolated products for every step (see below).

3.2.1. (2,2-dimethyl-1,3-dioxolan-4-yl)methyl 10-chlorodecanoate (**6**)

10-chlorodecanoyl chloride (SI-1, 1.10 g, 4.89 mmol, 1.0 equiv.) in

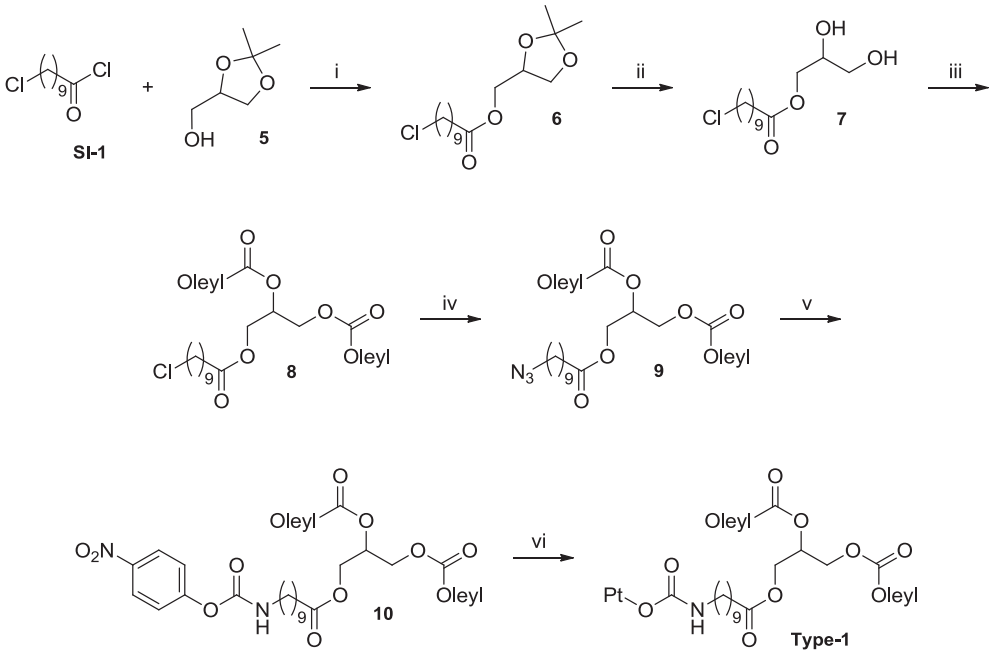

Scheme 1. Synthesis of Type-1 lipid mimetic prodrugs of pterostilbene. Reagents and conditions: i) **SI-1** (1.0 equiv.), **5** (1.8 equiv.), pyridine (2.8 equiv.), DCM, r.t. overnight, 90% isolated yield; ii) **6**, AcOH/H_2O 4:1 v/v, 50 °C for 35 min, 73% isolated yield; iii) oleoyl chloride (2.8 equiv.), **7** (1.0 equiv.), pyridine (3.0 equiv.), DCM, r.t. overnight, 99% isolated yield; iv) sodium azide (10.0 equiv.), **8** (1.0 equiv.), DMF, 60 °C overnight, 96% isolated yield; v) bis(4-nitrophenyl)carbonate (1.5 equiv.), 2,4,6-trimethylpyridine (2.0 equiv.), Lindlar catalyst (25% by wt.), **9** (1.0 equiv.), H_2, i-PrOH, 0 °C for 3 h, 75% isolated yield; vi) pterostilbene (3.0 equiv.), DMAP (3.0 equiv.), **10** (1.0 equiv.), THF, 50 °C for 18 h, 43% isolated yield.

DCM (5 mL) was added dropwise at 0 °C to a solution of DL-1,2-isopropylideneglycerol (**5**) (1.18 g, 8.94 mmol, 1.8 equiv.) and pyridine (1.08 g, 13.7 mmol, 2.8 equiv.) in DCM (12 mL), and the resulting solution was vigorously stirred at room temperature overnight. The reaction mixture was then diluted with DCM (50 mL) and washed with HCl 0.5 M (80 mL). The aqueous layer was extracted with DCM (3 × 50 mL) and the combined organic layers were dried over $MgSO_4$. The solvent was removed under reduced pressure and the oily residue was purified by flash chromatography (DCM/acetone 92:8, $R_f = 0.70$) to afford 1.42 g, 4.41 mmol of **6** (90% yield) as a slightly yellow oil. ^{1}H NMR (300 MHz, $CDCl_3$) δ 4.35–4.23 (m, 1H, -CH_2-C*H*-CH_2-), 4.20–4.00 (m, 3H, -C*H*$_2$-CH-C*H*$_2$-), 3.77–3.67 (m, 1H, -CH_2-CH-C*H*$_2$-), 3.51 (t, $J = 6.7$ Hz, 2H, -C*H*$_2$-Cl), 2.33 (t, $J = 7.5$ Hz, 2H, -C*H*$_2$-COO-), 1.82–1.68 (m, 2H, -C*H*$_2$-CH_2-Cl), 1.68–1.53 (m, 2H, -C*H*$_2$-CH_2-COO-), 1.47–1.19 (m, 16H, 2 × -C*H*$_3$ and 5 × -C*H*$_2$-). ^{13}C NMR (75 MHz, $CDCl_3$) δ 173.7, 109.9, 73.8, 66.5, 64.6, 45.2, 34.2, 32.7, 29.3, 29.2, 29.2, 28.9, 26.9, 26.8, 25.5, 25.0. ESI-MS (ESI+): 343 *m/z* $[M+Na]^+$, 359 *m/z* $[M+K]^+$.

3.2.2. 2,3-dihydroxypropyl 10-chlorodecanoate (*7*)

6 (1.36 g, 4.22 mmol) was dissolved in AcOH/H_2O 4:1 v/v (12 mL) and stirred at 50 °C for 35 min. The reaction mixture was then diluted with EtOAc (80 mL) and washed with a saturated solution of $NaHCO_3$ (adding solution until the production of gaseous CO_2 stopped). The aqueous layer was then extracted with EtOAc (2 × 50 mL) and the combined organic layers were dried over $MgSO_4$. The solvent was removed under reduced pressure and the oily residue was purified by flash chromatography (DCM/acetone 7:3, $R_f = 0.45$) to afford 0.87 g, 3.1 mmol of **7** (73% yield) as a colourless oil. ^{1}H NMR (300 MHz, $CDCl_3$) δ 4.23–4.09 (m, 2H, -COO-C*H*$_2$-CH-), 3.96–3.87 (m, 1H, -CH_2-C*H*-CH_2-), 3.73–3.55 (m, 2H, -CH-C*H*$_2$-OH), 3.52 (t, $J = 6.7$ Hz, 2H, -C*H*$_2$-Cl), 2.44 (br, 2H, 2 × -O*H*), 2.34 (t, $J = 7.5$ Hz, 2H, -C*H*$_2$-COO-), 1.82–1.69 (m, 2H, -C*H*$_2$-CH_2-Cl), 1.69–1.55 (m, 2H, -C*H*$_2$-CH_2-COO-), 1.48–1.21 (m, 10H, 5 × -C*H*$_2$-). ^{13}C NMR (75 MHz, $CDCl_3$) δ 174.4, 70.4, 65.3, 63.5, 45.3, 34.2, 32.7, 29.3, 29.2, 29.2, 28.9, 26.9, 25.0. ESI-MS (ESI+): 303 *m/z* $[M+Na]^+$.

3.2.3. (Z)-3-((10-chlorodecanoyl)oxy)propane-1,2-diyl dioleate (*8*)

Oleoyl chloride (purity 90%) (2.49 g, 8.27 mmol, 2.8 equiv.) in DCM (5 mL) was added dropwise at 0 °C to a solution of **7** (0.84 g, 3.0 mmol, 1.0 equiv.) and pyridine (0.70 g, 8.8 mmol, 3.0 equiv.) in DCM (20 mL) and the resulting solution was vigorously stirred at room temperature overnight. The reaction mixture was then diluted with DCM (25 mL) and washed with HCl 0.5 M (50 mL). The aqueous layer was extracted with DCM (2 × 25 mL) and the combined organic layers were dried over $MgSO_4$. The solvent was removed under reduced pressure and the oily residue was purified by flash chromatography (petroleum ether/acetone 95:5, $R_f = 0.23$) to afford 2.40 g, 2.97 mmol of **8** (99% yield) as a slightly yellow oil. ^{1}H NMR (300 MHz, $CDCl_3$) δ 5.42–5.20 (m, 5H, 2 × -C*H*=C*H*- and -CH_2-C*H*-CH_2-), 4.29 (dd, $J = 11.9$, 4.2 Hz, 2H, -C*H*$_2$-CH-C*H*$_2$-), 4.14 (dd, $J = 11.9$, 6.0 Hz, 2H, -C*H*$_2$-CH-C*H*$_2$-), 3.52 (t, $J = 6.7$ Hz, 2H, -C*H*$_2$-Cl), 2.31 (t, $J = 7.5$ Hz, 6H, 3 × -C*H*$_2$-COO-), 2.09–1.93 (m, 8H, 2 × -C*H*$_2$-CH=CH-C*H*$_2$-), 1.82–1.69 (m, 2H, -C*H*$_2$-CH_2-Cl), 1.68–1.53 (m, 6H, 3 × -C*H*$_2$-CH_2-COO-), 1.49–1.17 (m, 50H, 25 × -C*H*$_2$-), 0.92–0.83 (m, 6H, 2 × -C*H*$_3$). ^{13}C NMR (75 MHz, $CDCl_3$) δ 173.4, 173.4, 173.0, 130.2, 130.1, 129.8, 129.8, 69.0, 62.2, 45.3, 34.3, 34.2, 34.1, 32.8, 32.0, 29.9, 29.8, 29.7, 29.5, 29.4, 29.3, 29.3, 29.3, 29.3, 29.2, 29.2, 29.0, 27.4, 27.3, 27.0, 25.0, 25.0, 24.9, 22.8, 14.3. ESI-MS (ESI+): 827 *m/z* $[M + NH_4]^+$, 832 *m/z* $[M+Na]^+$, 848 *m/z* $[M+K]^+$.

3.2.4. (Z)-3-((10-azidodecanoyl)oxy)propane-1,2-diyl dioleate (*9*)

Sodium azide (1.90 g, 29.3 mmol, 10.0 equiv.) was added to a solution of **8** (2.37 g, 2.93 mmol, 1.0 equiv.) in anhydrous DMF (20 mL) and the resulting solution was stirred at 60 °C overnight. The reaction mixture was then diluted with EtOAc (60 mL) and washed with brine/H_2O 1:1 (6 × 30 mL). The organic layer was dried over $MgSO_4$, the solvent was removed under reduced pressure and the oily residue was purified by flash chromatography (petroleum ether/acetone 95:5, $R_f = 0.25$) to afford 2.30 g, 2.82 mmol of **9** (96% yield) as a slightly yellow oil. ^{1}H NMR (300 MHz, $CDCl_3$) δ 5.43–5.21 (m, 5H, 2 × -C*H*=C*H*- and -CH_2-C*H*-CH_2-), 4.29 (dd, $J = 11.9$, 4.2 Hz, 2H, -C*H*$_2$-CH-C*H*$_2$-), 4.14 (dd, $J = 11.9$, 5.9 Hz, 2H, -C*H*$_2$-CH-C*H*$_2$-), 3.25 (t, $J = 6.9$ Hz, 2H, -C*H*$_2$-N_3), 2.30 (t, $J = 7.5$ Hz, 6H, 3 × -C*H*$_2$-COO-), 2.07–1.94 (m, 8H, 2 × -C*H*$_2$-CH=CH-C*H*$_2$-), 1.67–1.53 (m, 8H, -C*H*$_2$-CH_2-N_3 and 3 × -C*H*$_2$-CH_2-COO-), 1.38–1.22 (m, 50H, 25 × -C*H*$_2$-), 0.91–0.83 (m, 6H, 2 × -C*H*$_3$). ^{13}C NMR (75 MHz, $CDCl_3$) δ 173.4, 173.3, 172.9, 130.2, 130.1, 129.8, 129.8, 69.0, 62.2, 51.6, 34.3, 34.2, 34.1, 32.0, 29.9, 29.9, 29.8, 29.7, 29.5, 29.4, 29.3, 29.3, 29.3, 29.2, 29.2, 29.2, 29.0, 27.4, 27.3, 26.8, 25.0, 25.0, 24.9, 22.8, 14.2. ESI-MS (ESI+): 834 *m/z* $[M + NH_4]^+$, 839 *m/z* $[M+Na]^+$.

3.2.5. (Z)-3-((10-(((4-nitrophenoxy)carbonyl)amino)decanoyl)oxy) propane-1,2-diyl dioleate (*10*)

Bis(4-nitrophenyl)carbonate (0.28 g, 0.92 mmol, 1.5 equiv.), 2,4,6-trimethylpyridine (0.15 g, 1.2 mmol, 2.0 equiv.) and Lindlar Catalyst (0.13 g, 25% by wt.) were added successively to a stirred solution of **9** (0.50 g, 0.61 mmol, 1.0 equiv.) in i-PrOH (15 mL). The reaction flask was evacuated and flushed with hydrogen gas. The resultant mixture was stirred under hydrogen at 0 °C for 3 h. After completion of the reaction, the catalyst was filtered through a pad of celite and the filter cake was washed with DCM (125 mL). The filtrate was washed with HCl 0.5 M (100 mL), the aqueous layer was extracted with DCM (50 mL) and the combined organic layers were dried over $MgSO_4$. The solvent was removed under reduced pressure and the oily residue was purified by flash chromatography (petroleum ether/acetone 85:15, $R_f = 0.33$) to afford 0.44 g, 0.46 mmol of **10** (75% yield) as a slightly yellow oil. ^{1}H NMR (300 MHz, $CDCl_3$) δ 8.22 (d, $J = 9.1$ Hz, 2H, Ar-*H*), 7.30 (d, $J = 9.1$ Hz, 2H, Ar-*H*), 5.40–5.16 (m, 5H, 2 × -C*H*=C*H*- and -CH_2-C*H*-CH_2-), 4.29 (dd, $J = 11.9$, 4.2 Hz, 2H, -C*H*$_2$-CH-C*H*$_2$-), 4.13 (dd, $J = 11.9$, 5.9 Hz, 2H, -C*H*$_2$-CH-C*H*$_2$-), 3.32–3.20 (m, 2H, -C*H*$_2$-NH-), 2.30 (t, $J = 7.3$ Hz, 6H, 3 × -C*H*$_2$-COO-), 2.07–1.90 (m, 8H, 2 × -C*H*$_2$-CH=CH-C*H*$_2$-), 1.67–1.51 (m, 8H, -C*H*$_2$-CH_2-NH- and 3 × -C*H*$_2$-CH_2-COO-), 1.42–1.13 (m, 50H, 25 × -C*H*$_2$-), 0.91–0.80 (m, 6H, 2 × -C*H*$_3$). ^{13}C NMR (75 MHz, $CDCl_3$) δ 173.4, 173.3, 172.9, 156.2, 153.2, 144.8, 130.1, 130.1, 129.8, 129.8, 125.2, 122.0, 69.0, 62.2, 41.5, 34.3, 34.1, 34.1, 32.0, 29.9, 29.8, 29.8, 29.6, 29.4, 29.4, 29.3, 29.3, 29.2, 29.2, 29.1, 29.1, 27.3, 27.3, 26.8, 25.0, 24.9, 24.9, 22.8, 14.2. ESI-MS (ESI+): 973 *m/z* $[M + NH_4]^+$, 978 *m/z* $[M+Na]^+$.

3.2.6. (Z) -3-((10-(((4-((E)-3,5-dimethoxystyryl)phenoxy)carbonyl) amino)decanoyl)oxy) propane-1,2-diyl dioleate (Type-1)

Pterostilbene (0.28 g, 1.1 mmol, 3.0 equiv.) and DMAP (0.13 g, 1.1 mmol, 3.0 equiv.) were added to a solution of **10** (0.35 g, 0.36 mmol, 1.0 equiv.) in HPLC grade THF (8.0 mL) and the resulting solution was stirred at 50 °C for 18 h. The reaction mixture was diluted with DCM (25 mL) and washed with HCl 0.5 M (50 mL). The aqueous layer was extracted with DCM (2 × 25 mL) and the combined organic layers were dried over $MgSO_4$. The solvent was removed under reduced pressure and the oily residue was purified twice by flash chromatography (1st: petroleum ether/acetone 8:2, $R_f = 0.40$; 2nd: DCM/acetone 99:1) to afford 0.17 g, 0.16 mmol of **Type-1** (43% yield) as a colourless oil. ^{1}H NMR (300 MHz, $CDCl_3$) δ 7.47 (d, $J = 8.4$ Hz, 2H, *H*-2′ and *H*-6′), 7.16–7.01 (m, 3H, Ar-C*H*=CH-Ar, *H*-3′ and *H*-5′), 6.96 (d, $J = 16.2$ Hz, 1H, Ar-CH=C*H*-Ar), 6.66 (m, 2H, *H*-2 and *H*-6), 6.41–6.37 (m, 1H, *H*-4), 5.41–5.22 (m, 5H, 2 × -C*H*=C*H*- and -CH_2-C*H*-CH_2-), 5.12–5.04 (m, 1H, -N*H*-), 4.30 (dd, $J = 11.9$, 4.2 Hz, 2H, -C*H*$_2$-CH-C*H*$_2$-), 4.14 (dd, $J = 11.9$, 5.9 Hz, 2H,

-CH_2-CH-CH_2-), 3.82 (s, 6H, 2 × -OCH_3), 3.30–3.20 (m, 2H, -CH_2-NH-), 2.36–2.26 (m, 6H, 3 × -CH_2-COO-), 2.07–1.94 (m, 8H, 2 × -CH_2-CH=CH-CH_2-), 1.68–1.51 (m, 8H, -CH_2-CH_2-NH- and 3 × -CH_2-CH_2-COO-), 1.40–1.18 (m, 50H, 25 × -CH_2-), 0.92–0.83 (m, 6H, 2 × -CH_3). ^{13}C NMR (75 MHz, $CDCl_3$) δ 173.4, 173.3, 172.9, 161.1, 154.5, 150.8, 139.4, 134.4, 130.1, 130.1, 129.8, 129.8, 128.6, 128.5, 127.5, 121.9, 104.7, 100.1, 69.0, 62.2, 55.5, 41.4, 34.3, 34.1, 34.1, 32.0, 29.9, 29.8, 29.8, 29.6, 29.4, 29.3, 29.3, 29.2, 29.2, 29.2, 29.2, 27.3, 27.3, 26.8, 25.0, 25.0, 24.9, 22.8, 14.2. ESI-MS (ESI+): 1073 m/z $[M + H]^+$, 1090 m/z $[M + NH_4]^+$, 1095 m/z $[M+Na]^+$, 1111 m/z $[M + K]^+$. Purity ≥95% (HPLC).

3.3. Synthesis of (Z)-2-((10-(((4-((E)-3,5-dimethoxystyryl) phenoxy)carbonyl) amino)decanoyl)oxy) propane-1,3-diyl dioleate (Type-2 prodrug)

The synthetic strategy adopted to synthesize the Type-2 lipid mimetic derivative of pterostilbene is similar to that developed for the Type-1 prodrug, but includes additional initial passages to synthesize the non-commercially available 1,3-isopropylidene protected glycerol (**SI-2**, See Supporting Information S4), which was obtained as described by Forbes et al. [52]. The subsequent passages in the synthesis are analogous to those described above for Type-1 prodrug (see Scheme 2).

3.3.1. 2,2-dimethyl-1,3-dioxan-5-yl 10-chlorodecanoate (**11**)

10-chlorodecanoyl chloride (**SI-1**, 1.33 g, 5.89 mmol, 1.2 equiv.) (see Supporting Information for its synthetic procedure) in DCM (5 mL) was added dropwise at 0 °C to a solution of **SI-2** (0.65 g, 4.9 mmol, 1.0 equiv.) and pyridine (0.59 g, 7.4 mmol, 1.5 equiv.) in DCM (10 mL), and the resulting solution was vigorously stirred at room temperature overnight. The reaction mixture was then diluted with DCM (25 mL) and washed with HCl 0.5 M (40 mL). The aqueous layer was extracted with DCM (3 × 25 mL) and the combined organic layers were dried over $MgSO_4$. The solvent was removed under reduced pressure and the oily residue was purified by flash chromatography (DCM/acetone 92:8, R_f = 0.72) to afford 1.47 g, 4.57 mmol of **11** (93% yield) as a slightly yellow oil. ^{1}H NMR (300 MHz, $CDCl_3$) δ 4.73–4.64 (m, 1H, -CH_2-C*H*-CH_2-), 4.07 (dd, J = 12.9, 3.3 Hz, 2H, -CH_2-CH-CH_2-), 3.78 (dd, J = 13.0, 3.5 Hz, 2H, -CH_2-CH-CH_2-), 3.50 (t, J = 6.7 Hz, 2H, -CH_2-Cl), 2.35 (t, J = 7.5 Hz, 2H, -CH_2-COO-), 1.80–1.68 (m, 2H, -CH_2-CH_2-Cl), 1.68–1.53 (m, 2H, -CH_2-CH_2-COO-), 1.47–1.20 (m, 16H, 2 × -CH_3 and 5 × -CH_2-). ^{13}C NMR (75 MHz, $CDCl_3$) δ 173.6, 98.5, 66.0, 62.6, 62.1, 45.2, 34.4, 32.7, 29.3, 29.2, 29.1, 28.9, 26.9, 26.2, 25.0, 21.1. ESI-MS (ESI+): 343 m/z $[M + Na]^+$.

3.3.2. 1,3-dihydroxypropan-2-yl 10-chlorodecanoate (**12**)

11 (1.42 g, 4.42 mmol) was dissolved in AcOH/H_2O 4:1 v/v (13 mL) and stirred at 50 °C for 35 min. The reaction mixture was then diluted with EtOAc (80 mL) and washed with a saturated solution of $NaHCO_3$ (adding the solution until the production of gaseous CO_2 stopped). The aqueous layer was then extracted with EtOAc (2 × 50 mL) and the combined organic layers were dried over $MgSO_4$. The solvent was removed under reduced pressure and the oily residue was purified by flash chromatography (DCM/acetone 7:3, R_f = 0.43) to afford 1.08 g, 3.84 mmol of **12** (87% yield) as a colourless oil. ^{1}H NMR (300 MHz, $CDCl_3$) δ 4.94–4.84 (m, 1H, -CH_2-C*H*-CH_2-), 3.85–3.73 (m, 4H, -CH_2-CH-CH_2-), 3.51 (t, J = 6.7 Hz, 2H, -CH_2-Cl), 2.67 (br, 2H, 2 × -O*H*), 2.35 (t, J = 7.3 Hz, 2H, -CH_2-COO-), 1.80–1.68 (m, 2H, -CH_2-CH_2-Cl), 1.68–1.54 (m, 2H, -CH_2-CH_2-COO-), 1.47–1.22 (m, 10H, 5 × -CH_2-). ^{13}C NMR (75 MHz, $CDCl_3$) δ 174.2, 75.0, 62.3, 45.2, 34.4, 32.7, 29.3, 29.2, 29.1, 28.9, 26.9, 25.0. ESI-MS (ESI+): 303 m/z $[M + Na]^+$.

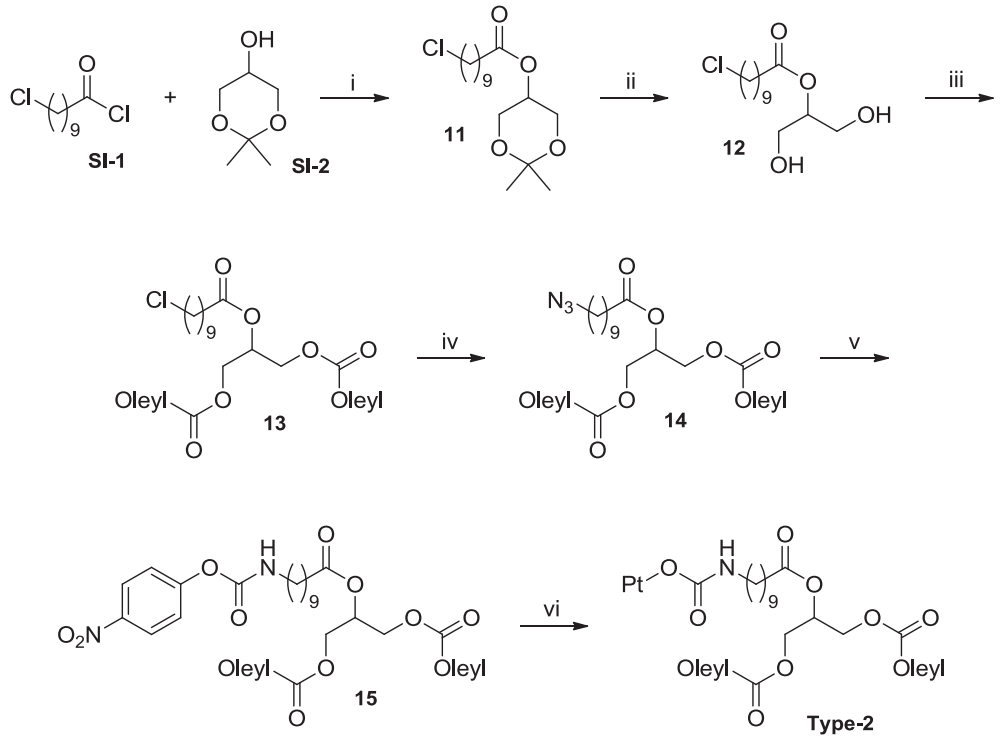

Scheme 2. Synthesis of Type-2 lipid mimetic prodrugs of pterostilbene. Reagents and conditions: i) **SI-1** (1.2 equiv.), **SI-2** (1.0 equiv.), pyridine (1.5 equiv.), DCM, r.t. overnight, 93% isolated yield; ii) **11**, AcOH/H_2O 4:1 v/v, 50 °C for 35 min, 87% isolated yield; iii) oleoyl chloride (2.5 equiv.), **12** (1.0 equiv.), pyridine (3.1 equiv.), DCM, r.t. overnight, 98% isolated yield; iv) sodium azide (10.0 equiv.), **13** (1.0 equiv.), DMF, 60 °C overnight, 97% isolated yield; v) bis(4-nitrophenyl)carbonate (1.5 equiv.), 2,4,6-trimethylpyridine (2.0 equiv.), Lindlar catalyst (25% by wt.), **14** (1.0 equiv.), H_2, i-PrOH, 0 °C for 3 h, 77% isolated yield; vi) pterostilbene (3.0 equiv.), DMAP (3.0 equiv.), **15** (1.0 equiv.), THF, 50 °C for 18 h, 46% isolated yield.

*3.3.3. (Z)-2-((10-chlorodecanoyl)oxy)propane-1,3-diyl dioleate (**13**)*

Oleoyl chloride (purity 90%) (2.99 g, 8.94 mmol, 2.5 equiv.) in DCM (6 mL) was added dropwise at 0 °C to a solution of **12** (1.00 g, 3.57 mmol, 1.0 equiv.) and pyridine (0.85 g, 11 mmol, 3.1 equiv.) in DCM (25 mL) and the resulting solution was vigorously stirred at room temperature overnight. The reaction mixture was then diluted with DCM (30 mL) and washed with HCl 0.5 M (60 mL). The aqueous layer was extracted with DCM (2 × 30 mL) and the combined organic layers were dried over $MgSO_4$. The solvent was removed under reduced pressure and the oily residue was purified by flash chromatography (petroleum ether/acetone 95:5, $R_f = 0.21$) to afford 2.85 g, 3.52 mmol of **13** (98% yield) as a slightly yellow oil. ^{1}H NMR (300 MHz, $CDCl_3$) δ 5.42–5.20 (m, 5H, 2 × -C*H*=C*H*- and -CH_2-C*H*-CH_2-), 4.29 (dd, *J* = 11.9, 4.2 Hz, 2H, -C*H*$_2$-CH-C*H*$_2$-), 4.14 (dd, *J* = 11.9, 5.9 Hz, 2H, -C*H*$_2$-CH-C*H*$_2$-), 3.52 (t, *J* = 6.7 Hz, 2H, -C*H*$_2$-Cl), 2.31 (t, *J* = 7.5 Hz, 6H, 3 × -C*H*$_2$-COO-), 2.09–1.91 (m, 8H, 2 × -C*H*$_2$-CH=CH-C*H*$_2$-), 1.83–1.69 (m, 2H, -C*H*$_2$-CH_2-Cl), 1.68–1.53 (m, 6H, 3 × -C*H*$_2$-CH_2-COO-), 1.49–1.16 (m, 50H, 25 × -C*H*$_2$-), 0.88 (t, *J* = 6.3 Hz, 6H, 2 × -C*H*$_3$). ^{13}C NMR (75 MHz, $CDCl_3$) δ 173.4, 172.9, 130.1, 129.8, 69.0, 62.2, 45.2, 34.3, 34.2, 32.7, 32.0, 29.9, 29.8, 29.7, 29.5, 29.4, 29.3, 29.3, 29.2, 29.2, 29.2, 29.1, 29.0, 27.4, 27.3, 27.0, 25.0, 22.8, 14.3. ESI-MS (ESI+): 827 *m*/*z* $[M + NH_4]^+$, 832 *m*/*z* $[M + Na]^+$, 848 *m*/*z* $[M + K]^+$.

*3.3.4. (Z)-2-((10-azidodecanoyl)oxy)propane-1,3-diyl dioleate (**14**)*

Sodium azide (2.24 g, 34.4 mmol, 10.0 equiv.) was added to a solution of **13** (2.79 g, 3.44 mmol, 1.0 equiv.) in dry DMF (25 mL) and the resulting solution was stirred at 60 °C overnight. The reaction mixture was then diluted with EtOAc (70 mL) and washed with brine/H_2O 1:1 (6 × 35 mL). The organic layer was dried over $MgSO_4$, the solvent was removed under reduced pressure and the oily residue was purified by flash chromatography (petroleum ether/acetone 95:5, $R_f = 0.25$) to afford 2.73 g, 3.34 mmol of **14** (97% yield) as a slightly yellow oil. ^{1}H NMR (300 MHz, $CDCl_3$) δ 5.45–5.20 (m, 5H, 2 × -C*H*=C*H*- and -CH_2-C*H*-CH_2-), 4.29 (dd, *J* = 11.9, 4.3 Hz, 2H, -C*H*$_2$-CH-C*H*$_2$-), 4.14 (dd, *J* = 11.9, 5.9 Hz, 2H, -C*H*$_2$-CH-C*H*$_2$-), 3.25 (t, *J* = 6.9 Hz, 2H, -C*H*$_2$-N_3), 2.36–2.26 (m, 6H, 3 × -C*H*$_2$-COO-), 2.07–1.95 (m, 8H, 2 × -C*H*$_2$-CH=CH-C*H*$_2$-), 1.67–1.52 (m, 8H, -C*H*$_2$-CH_2-N_3 and 3 × -C*H*$_2$-CH_2-COO-), 1.38–1.20 (m, 50H, 25 × -C*H*$_2$-), 0.87 (t, *J* = 6.6 Hz, 6H, 2 × -C*H*$_3$). ^{13}C NMR (75 MHz, $CDCl_3$) δ 173.3, 172.9, 130.1, 129.8, 69.0, 62.2, 51.6, 34.3, 34.2, 32.0, 29.9, 29.8, 29.7, 29.5, 29.4, 29.3, 29.3, 29.2, 29.2, 29.2, 29.1, 29.0, 27.4, 27.3, 26.8, 25.0, 22.8, 14.2. ESI-MS (ESI+): 834 *m*/*z* $[M + NH_4]^+$, 839 *m*/*z* $[M + Na]^+$.

*3.3.5. (Z)-2-((10-(((4-nitrophenoxy)carbonyl)amino)decanoyl)oxy) propane-1,3-diyl dioleate (**15**)*

Bis(4-nitrophenyl)carbonate (0.28 g, 0.92 mmol, 1.5 equiv.), 2,4,6-trimethylpyridine (0.15 g, 1.2 mmol, 2.0 equiv.) and Lindlar catalyst (0.13 g, 25% by wt.) were added successively to a stirred solution of **14** (0.51 g, 0.62 mmol, 1.0 equiv.) in i-PrOH (15 mL). The reaction flask was evacuated and flushed with hydrogen gas. The resultant mixture was stirred under hydrogen at 0 °C for 3 h. After completion of the reaction, the catalyst was filtered through a pad of celite and the filter cake was washed with DCM (125 mL). The filtrate was washed with HCl 0.5 M (100 mL), the aqueous layer was extracted with DCM (50 mL) and the combined organic layers were dried over $MgSO_4$. The solvent was removed under reduced pressure and the oily residue was purified by flash chromatography (petroleum ether/acetone 85:15, R_f = 0.31) to afford 0.46 g, 0.48 mmol of **15** (77% yield) as a slightly yellow oil. ^{1}H NMR (300 MHz, $CDCl_3$) δ 8.22 (d, *J* = 9.0 Hz, 2H, Ar-*H*), 7.30 (d, *J* = 9.0 Hz, 2H, Ar-*H*), 5.41–5.16 (m, 5H, 2 × -C*H*=C*H*- and -CH_2-C*H*-CH_2-), 4.29 (dd, *J* = 11.8, 4.3 Hz, 2H, -C*H*$_2$-CH-C*H*$_2$-), 4.14 (dd, *J* = 11.9, 5.8 Hz, 2H, -C*H*$_2$-CH-C*H*$_2$-), 3.32–3.21 (m, 2H, -C*H*$_2$-NH-), 2.30 (t, *J* = 7.5 Hz, 6H, 3 × -C*H*$_2$-COO-), 2.08–1.91 (m, 8H, 2 × -C*H*$_2$-CH=CH-C*H*$_2$-), 1.68–1.50 (m, 8H, -C*H*$_2$-CH_2-NH- and 3 × -C*H*$_2$-CH_2-COO-), 1.42–1.17 (m, 50H, 25 × -C*H*$_2$-), 0.93–0.80 (m, 6H, 2 × -C*H*$_3$). ^{13}C NMR (75 MHz, $CDCl_3$) δ 173.3, 172.9, 156.1, 153.2, 144.8, 130.1, 129.8, 125.2, 122.0, 69.0, 62.2, 41.5, 34.2, 34.1, 32.0, 29.9, 29.8, 29.8, 29.6, 29.4, 29.4, 29.3, 29.3, 29.2, 29.2, 29.1, 27.3, 27.3, 26.8, 24.9, 24.9, 22.8, 14.2. ESI-MS (ESI+): 973 *m*/*z* $[M + NH_4]^+$, 978 *m*/*z* $[M + Na]^+$.

3.3.6. (Z) -2-((10-(((4-((E)-3,5-dimethoxystyryl)phenoxy)carbonyl) amino)decano yl)oxy) propane-1,3-diyl dioleate (Type-2)

Pterostilbene (0.30 g, 1.2 mmol, 3.0 equiv.) and DMAP (0.14 g, 1.2 mmol, 3.0 equiv.) were added to a solution of **15** (0.37 g, 0.39 mmol, 1.0 equiv.) in HPLC-grade THF (8.0 mL) and the resulting solution was stirred at 50 °C for 18 h. The reaction mixture was diluted with DCM (25 mL) and washed with HCl 0.5 M (50 mL). The aqueous layer was extracted with DCM (2 × 25 mL) and the combined organic layers were dried over $MgSO_4$. The solvent was removed under reduced pressure and the oily residue was purified two times by flash chromatography (1st: petroleum ether/acetone 8:2, $R_f = 0.39$; 2nd: DCM/acetone 99:1) to afford 0.19 g, 0.18 mmol of **Type-2** (46% yield) as a white solid. ^{1}H NMR (300 MHz, $CDCl_3$) δ 7.47 (d, *J* = 8.5 Hz, 2H, *H*-2′ and *H*-6′), 7.17–7.01 (m, 3H, Ar-C*H*=CH-Ar, *H*-3′ and *H*-5′), 6.96 (d, *J* = 16.2 Hz, 1H, Ar-CH=C*H*-Ar), 6.66 (d, *J* = 2.1 Hz, 2H, *H*-2 and *H*-6), 6.39 (t, *J* = 2.0 Hz, 1H, *H*-4), 5.42–5.21 (m, 5H, 2 × -C*H*=C*H*- and -CH_2-C*H*-CH_2-), 5.11–5.01 (m, 1H, -N*H*-), 4.30 (dd, *J* = 11.9, 4.3 Hz, 2H, -C*H*$_2$-CH-C*H*$_2$-), 4.15 (dd, *J* = 11.9, 5.9 Hz, 2H, -C*H*$_2$-CH-C*H*$_2$-), 3.82 (s, 6H, 2 × -OC*H*$_3$), 3.33–3.19 (m, 2H, -C*H*$_2$-NH-), 2.37–2.24 (m, 6H, 3 × -C*H*$_2$-COO-), 2.09–1.91 (m, 8H, 2 × -C*H*$_2$-CH=CH-C*H*$_2$-), 1.68–1.50 (m, 8H, -C*H*$_2$-CH_2-NH- and 3 × -C*H*$_2$-CH_2-COO-), 1.38–1.21 (m, 50H, 25 × -C*H*$_2$-), 0.91–0.83 (m, 6H, 2 × -C*H*$_3$). ^{13}C NMR (75 MHz, $CDCl_3$) δ 173.4, 172.9, 161.1, 154.6, 150.8, 139.4, 134.4, 130.1, 129.8, 128.7, 128.5, 127.5, 121.9, 104.7, 100.1, 69.0, 62.2, 55.5, 41.4, 34.3, 34.1, 32.0, 29.9, 29.8, 29.6, 29.4, 29.4, 29.3, 29.3, 29.2, 29.2, 29.1, 27.3, 27.3, 26.8, 25.0, 22.8, 14.2. ESI-MS (ESI+): 1073 *m*/*z* $[M + H]^+$, 1090 *m*/*z* $[M + NH_4]^+$, 1095 *m*/*z* $[M + Na]^+$, 1111 *m*/*z* $[M + K]^+$. Purity ≥95% (HPLC).

3.4. HPLC-UV analysis

Samples (2 μL) were analyzed by HPLC-UV (1290 Infinity LC System, Agilent Technologies) using a reverse phase column and a UV diode array detector (190–500 nm). Type-1, Type-2 prodrugs and their hydrolysis products were analyzed with a Zorbax Extend-C18 column (Rapid Resolution HT, 1.8 μm, 50 × 3.0 mm i.d.; Agilent Technologies, cat. n. 727975-302); solvents A and B were water containing 0.1% trifluoroacetic acid (TFA) and THF/MeCN 7:3, respectively. The gradient for B was as follows: 30% for 0.5 min, then from 30% to 100% in 6.5 min, 100% for 3 min; the flow rate was 0.5 mL/min and column compartment was maintained at 50 °C. Pterostilbene and its phase II metabolites were analyzed with a Zorbax Eclipse Plus C18 column (Rapid Resolution HD, 1.8 μm, 50 × 2.1 mm i.d.; Agilent Technologies, cat. n. 959757-902); solvents A and B were water containing 0.1% trifluoroacetic acid (TFA) and MeCN, respectively. The gradient for B was as follows: 10% for 0.5 min, then from 10% to 100% in 3.5 min, 100% for 1 min; the flow rate was 0.6 mL/min and column compartment was maintained at 35 °C. In both cases the eluate was preferentially monitored at 286, 300 and 320 nm (corresponding to absorbance maxima of the internal standard, derivatives/metabolites and pterostilbene, respectively).

3.5. HPLC/ESI-MS analysis

HPLC/ESI-MS analysis was performed on selected samples

(20 μL) with a 1100 Series system (Agilent Technologies) using a reversed phase column (Zorbax Eclipse XDB-C18, 5 μm, 150 × 4.6 mm i.d.; Agilent Technologies, cat. n. 993967-902). Solvents A and B were water +0.1% formic acid and MeCN +0.1% formic acid, respectively. The gradient for B was as follows: from 30% to 100% in 18 min, then 100% for 7 min; the flow rate was 0.7 mL/min. The eluate was preferentially monitored at 286, 300 and 320 nm. MS analysis was performed with an ESI source operating in full-scan positive ion mode, applying the following ESI parameters: nebulizer pressure 50 psi, dry gas flow 8 l/min, dry gas temperature 350 °C.

3.6. Pancreatic lipase assays

The assay medium, meant to simulate intestinal physiological conditions, was prepared adding 0.3 mg of lipase from porcine pancreas (Type VI-S, Sigma, cat. n. L0382) and 155 μL of colipase (Sigma, cat. n. C3028) from porcine pancreas (1 mg/mL solution in Milli-Q water) to 8.85 mL of a 0.016 M $CaCl_2$, 0.02% sodium taurodeoxycholate hydrate, 0.1 M TRIS·HC1 (pH 7.7) buffer solution. Lipolysis was started by adding 40 μL of Type-1 or Type-2 prodrug (10 mM stock solutions in THF) to two vials containing 3.96 mL of the assay medium previously warmed at 37 °C. The solutions were stirred vigorously at 37 °C. The reactions were stopped at selected time points by dilution of 200 μL of the reaction mixtures in 300 μL of THF, which was shown to inactivate PL. HPLC/UV analysis (300–320 nm) of the resulting cleared solutions detected Pt-containing species (i.e. Type-1 and -2 derivatives, hydrolysis products containing pterostilbene and pterostilbene itself). Peak areas in the chromatograms were determined and normalized to the total area of the peaks in each chromatogram, assuming that all analytes have the same molar extinction coefficient. Control experiments established that the rate of hydrolysis after inactivation of PL was negligible.

3.7. Animals

C57BL mice from the facility of the Department of Biomedical Sciences were used for pharmacokinetic experiments. All experiments involving animals were performed after approval by the University of Padova Ethical Committee for Animal Welfare (OPBA) and by the Italian Ministry of Health (Permit Number 211/2015-PR), and with the supervision of the Central Veterinary Service of the University of Padova, in compliance with Italian Law DL 26/2014, embodying UE Directive 2010/63/EU.

3.8. Tissue extraction

Pterostilbene, pterostilbene-sulfate and pterostilbene-glucuronide were extracted and quantified from blood and tissues (brain, heart, kidneys, liver and lungs) as described in Azzolini et al. [34]. Recovery yields of pterostilbene-glucuronide from blood and tissues were assumed to be the same as for pterostilbene-sulfate [34]. Adequate recovery yields from adipose tissue were obtained modifying the extraction protocol as follows: 1 g of adipose tissue was mixed with 1 mL of D-PBS (Euroclone), and homogenized with a motorized polypropylene pestel (Sigma) or with an Ultra-Turrax T25 homogenizer (Janke & Kunkel). 200 mg of tissue homogenate were transferred into a vial and spiked with the internal standard (4,4'-dihydroxybiphenyl, dilution from a 50× stock solution in MeCN, 25 nmol/g tissue final concentration). 10 μL of 4.35 M acetic acid and 900 μL of acetone were added. Samples were vortexed (2 min), sonicated (30 min), stirred overnight at 4 °C and then centrifuged (12,000 g, 7 min, 4 °C). An accurately measured portion of the supernatant was finally collected and stored at −20 °C. Before analysis, acetone was allowed to evaporate at room temperature using a Univapo 150H (UniEquip) vacuum concentrator centrifuge, and up to 40 μL of acetone were added to precipitate residual proteins; after centrifugation (12,000 g, 5 min, 4 °C), cleared samples were analyzed by HPLC/UV. Recovery yields of pterostilbene and Pt-sulfate from adipose tissue were determined processing tissue (from an untreated animal) spiked with a known amount of pterostilbene or Pt-sulfate (1 g of tissue mixed with 1 mL of PBS containing 5 nmoles of the compound). Recovery yield of Pt-glucuronide was assumed to be the same of Pt-sulfate.

A different extraction protocol was used to extract Type-1 and Type-2 derivatives from adipose tissue: 100 mg of adipose tissue were mixed with 10 mL $CHCl_3$ and homogenized using an Ultra-Turrax T25 homogenizer (Janke & Kunkel). 10 mL of MeOH were added, the sample was further homogenized and then transferred into a separatory funnel, washing the tube with 10 mL $CHCl_3$. 10 mL ultrapure water were added, and extraction with 10 mL $CHCl_3$ was repeated twice. The organic phase was evaporated under vacuum, and the sample was resuspended in 100 μL THF and analyzed by HPLC/UV.

3.9. Tissue distribution studies

Mice were fed with a high fat diet (60% calories from fat; OpenSource Diets, cat. n. D12492) for 6 weeks (starting from day 21). Pterostilbene, Type-1 or Type-2 were then added to the diet for 2 weeks (1 μmol/g diet, corresponding approximatively to 176 μmol/kg body weight/day). At the end of the treatment, animals were anesthetized with isoflurane and sacrificed (N = 6 for each condition). Blood was collected in heparinized tubes, kept in ice and treated as described above within 10 min. Brain, heart, kidneys, liver, lungs, visceral adipose tissue and subcutaneous adipose tissue were explanted, weighed and immediately frozen in liquid nitrogen. 1 g of thawed tissue was treated as described above for extraction of pterostilbene and its metabolites. Adipose tissue (only) was treated also with the protocol for extraction of Type-1 and Type-2 derivatives.

Author contribution

A.M., C.P., M.Z., L.B. designed the study and wrote the manuscript; A.M., A.R., V.B. carried out the syntheses; A.M., A.R. performed the hydrolysis studies; V.B., M.A., M.L.S. performed *in vivo* experiments. All authors reviewed the manuscript.

Author disclosure statement

The authors report no conflicts of interest.

Acknowledgments

This work was supported by the CNR Project of Special Interest on Aging and by grants from the Italian Ministry of the University and Research (PRIN n. 20107Z8XBW_004 and PRONAT project) and from Regione Veneto- European Social Fund (project n. 436-2-2121-2015). M.A. gratefully acknowledges support by a fellowship from Fondazione Umberto Veronesi. A.M acknowledges support by a senior research grant from University of Padova, DR. 3210-2013.

Appendix A. Supplementary data

Supplementary data related to this article can be found at http://dx.doi.org/10.1016/j.ejmech.2017.04.034.

List of abbreviations

AcOH	acetic acid
AMPK	5′ AMP-activated protein kinase
APC	active phenolic compound
ARE	antioxidant response elements
BAT	brown adipose tissue
CNS	central nervous system
CVD	cardiovascular disease
DCM	dichloromethane
DMAP	4-Dimethylaminopyridine
DMF	*N*,*N*-Dimethylformamide
Et_2O	diethyl ether
EtOAc	ethyl acetate
FA	fatty acid
IL	interleukin
iNOS	inducible NO-synthase
i-PrOH	isopropanol
Keap1	Kelch-like ECH-associated protein 1
LP	lipoprotein
LPL	lipoprotein lipase
MeCN	acetonitrile
MeOH	methanol
MsCl	methanesulfonyl chloride
Nrf2	Nuclear factor erythroid 2-related factor 2
PCC	pyridinium chlorochromate
PL	pancreatic lipase
PTSA	p-Toluenesulfonic acid
ROS	reactive oxygen species
r.t.	room temperature
T2D	type 2 diabetes
TEA	triethylamine
THF	tetrahydrofuran
TNFα	Tumor necrosis factor alpha
UCP1	Uncoupling Protein 1
WAT	white adipose tissue

References

[1] S.D. Malnick, H. Knobler, The medical complications of obesity, QJM Mon. J. Assoc. Physicians 99 (2006) 565–579.
[2] A. Hruby, J.E. Manson, L. Qi, V.S. Malik, E.B. Rimm, Q. Sun, W.C. Willett, F.B. Hu, Determinants and consequences of obesity, Am. J. Public Health 106 (2016) 1656–1662.
[3] M.V. Abranches, F.C. Oliveira, L.L. Conceicao, M.D. Peluzio, Obesity and diabetes: the link between adipose tissue dysfunction and glucose homeostasis, Nutr. Res. Rev. 28 (2015) 121–132.
[4] D.W. Lam, D. LeRoith, Metabolic syndrome, in: L.J. De Groot, G. Chrousos, K. Dungan, K.R. Feingold, A. Grossman, J.M. Hershman, C. Koch, M. Korbonits, R. McLachlan, M. New, J. Purnell, R. Rebar, F. Singer, A. Vinik (Eds.), Endotext, MDText.com, Inc., South Dartmouth (MA), 2000.
[5] M. Fasshauer, M. Bluher, Adipokines in health and disease, Trends Pharmacol. Sci. 36 (2015) 461–470.
[6] P. Bhargava, C.H. Lee, Role and function of macrophages in the metabolic syndrome, Biochem. J. 442 (2012) 253–262.
[7] T. Ruskovska, D.A. Bernlohr, Oxidative stress and protein carbonylation in adipose tissue - implications for insulin resistance and diabetes mellitus, J. Proteom. 92 (2013) 323–334.
[8] C.Y. Han, Roles of reactive oxygen species on insulin resistance in adipose tissue, Diabetes Metab. J. 40 (2016) 272–279.
[9] S.H. Chin, C.N. Kahathuduwa, M. Binks, Physical activity and obesity: what we know and what we need to know, Obes. Rev. 17 (2016) 1226–1244.
[10] J.P. Thyfault, D.C. Wright, "Weighing" the effects of exercise and intrinsic aerobic capacity: are there beneficial effects independent of changes in weight? Appl. Physiol. Nutr. Metab. 41 (2016) 911–916.
[11] N. Jeremic, P. Chaturvedi, S.C. Tyagi, Browning of white fat: novel insight into factors, mechanisms, and therapeutics, J. Cell. Physiol. 232 (2017) 61–68.
[12] K.I. Stanford, R.J. Middelbeek, L.J. Goodyear, Exercise effects on white adipose tissue: beiging and metabolic adaptations, Diabetes 64 (2015) 2361–2368.
[13] A.L. Poher, J. Altirriba, C. Veyrat-Durebex, F. Rohner-Jeanrenaud, Brown adipose tissue activity as a target for the treatment of obesity/insulin resistance, Front. Physiol. 6 (2015) 4.
[14] F. Villarroya, R. Cereijo, J. Villarroya, M. Giralt, Brown adipose tissue as a secretory organ, Nat. Rev. Endocrinol. 13 (2017) 26–35.
[15] A.D. van Dam, S. Kooijman, M. Schilperoort, P.C. Rensen, M.R. Boon, Regulation of brown fat by AMP-activated protein kinase, Trends Mol. Med. 21 (2015) 571–579.
[16] J.D. Gotthardt, N.T. Bello, Can we win the war on obesity with pharmacotherapy? Expert Rev. Clin. Pharmacol. 9 (2016) 1–9.
[17] R. Khera, M.H. Murad, A.K. Chandar, P.S. Dulai, Z. Wang, L.J. Prokop, R. Loomba, M. Camilleri, S. Singh, Association of pharmacological treatments for obesity with weight loss and adverse events: a systematic review and meta-analysis, JAMA 315 (2016) 2424–2434.
[18] X.R. Peng, P. Gennemark, G. O'Mahony, S. Bartesaghi, Unlock the thermogenic potential of adipose tissue: pharmacological modulation and implications for treatment of diabetes and obesity, Front. Endocrinol. 6 (2015) 174.
[19] Long-term safety, tolerability, and weight loss associated with metformin in the diabetes prevention program outcomes study, Diabetes Care 35 (2012) 731–737.
[20] J. Martel, D.M. Ojcius, C.J. Chang, C.S. Lin, C.C. Lu, Y.F. Ko, S.F. Tseng, H.C. Lai, J.D. Young, Anti-obesogenic and antidiabetic effects of plants and mushrooms, Nat. Rev. Endocrinol. 13 (2017) 149–160.
[21] M. Castro, M. Preto, V. Vasconcelos, R. Urbatzka, Obesity: the metabolic disease, advances on drug discovery and natural product research, Curr. Top. Med. Chem. 16 (2016) 2577–2604.
[22] M.C. Crespo, F. Visioli, A brief review of blue- and bilberries' potential to curb cardio-metabolic perturbations: focus on diabetes, Curr. Pharm. Des. 22 (2016), http://dx.doi.org/10.2174/1381612822666161010120523.
[23] M. Gasparrini, F. Giampieri, J.M. Alvarez Suarez, L. Mazzoni, Y.F.H. T, L.Q. J, P. Bullon, M. Battino, AMPK as a new attractive therapeutic target for disease prevention: the role of dietary compounds AMPK and disease prevention, Curr. Drug Targets 17 (2016) 865–889.
[24] S. Timmers, E. Konings, L. Bilet, R.H. Houtkooper, T. van de Weijer, G.H. Goossens, J. Hoeks, S. van der Krieken, D. Ryu, S. Kersten, E. Moonen-Kornips, M.K. Hesselink, I. Kunz, V.B. Schrauwen-Hinderling, E.E. Blaak, J. Auwerx, P. Schrauwen, Calorie restriction-like effects of 30 days of resveratrol supplementation on energy metabolism and metabolic profile in obese humans, Cell Metab. 14 (2011) 612–622.
[25] T. Szkudelski, K. Szkudelska, Resveratrol and diabetes: from animal to human studies, Biochim. Biophys. Acta 1852 (2015) 1145–1154.
[26] S. Wang, X. Liang, Q. Yang, X. Fu, C.J. Rogers, M. Zhu, B.D. Rodgers, Q. Jiang, M.V. Dodson, M. Du, Resveratrol induces brown-like adipocyte formation in white fat through activation of AMP-activated protein kinase (AMPK) alpha1, Int. J. Obes. Lond. 39 (2015) 967–976.
[27] M. Reinisalo, A. Karlund, A. Koskela, K. Kaarniranta, R.O. Karjalainen, Polyphenol stilbenes: molecular mechanisms of defence against oxidative stress and aging-related diseases, Oxidative Med. Cell. Longev. 2015 (2015) 340520.
[28] J.M. Andrade, A.C. Frade, J.B. Guimaraes, K.M. Freitas, M.T. Lopes, A.L. Guimaraes, A.M. de Paula, C.C. Coimbra, S.H. Santos, Resveratrol increases brown adipose tissue thermogenesis markers by increasing SIRT1 and energy expenditure and decreasing fat accumulation in adipose tissue of mice fed a standard diet, Eur. J. Nutr. 53 (2014) 1503–1510.
[29] E. Wenzel, V. Somoza, Metabolism and bioavailability of trans-resveratrol, Mol. Nutr. Food Res. 49 (2005) 472–481.
[30] D. McCormack, D. McFadden, A review of pterostilbene antioxidant activity and disease modification, Oxidative Med. Cell. Longev. 2013 (2013) 575482.
[31] J.M. Estrela, A. Ortega, S. Mena, M.L. Rodriguez, M. Asensi, Pterostilbene: biomedical applications, Crit. Rev. Clin. Lab. Sci. 50 (2013) 65–78.
[32] R. Kosuru, U. Rai, S. Prakash, A. Singh, S. Singh, Promising therapeutic potential of pterostilbene and its mechanistic insight based on preclinical evidence, Eur. J. Pharmacol. 789 (2016) 229–243.
[33] I.M. Kapetanovic, M. Muzzio, Z. Huang, T.N. Thompson, D.L. McCormick, Pharmacokinetics, oral bioavailability, and metabolic profile of resveratrol and its dimethylether analog, pterostilbene, in rats, Cancer Chemother. Pharmacol. 68 (2011) 593–601.
[34] M. Azzolini, M. La Spina, A. Mattarei, C. Paradisi, M. Zoratti, L. Biasutto, Pharmacokinetics and tissue distribution of pterostilbene in the rat, Mol. Nutr. Food Res. 58 (2014) 2122–2132.
[35] Y.S. Chiou, M.L. Tsai, K. Nagabhushanam, Y.J. Wang, C.H. Wu, C.T. Ho, M.H. Pan, Pterostilbene is more potent than resveratrol in preventing azoxymethane (AOM)-induced colon tumorigenesis via activation of the NF-E2-related factor 2 (Nrf2)-mediated antioxidant signaling pathway, J. Agric. Food Chem. 59 (2011) 2725–2733.
[36] J. Chang, A. Rimando, M. Pallas, A. Camins, D. Porquet, J. Reeves, B. Shukitt-Hale, M.A. Smith, J.A. Joseph, G. Casadesus, Low-dose pterostilbene, but not resveratrol, is a potent neuromodulator in aging and Alzheimer's disease, Neurobiol. Aging 33 (2012) 2062–2071.
[37] M. Azzolini, A. Mattarei, M. La Spina, M. Fanin, G. Chiodarelli, M. Romio, M. Zoratti, C. Paradisi, L. Biasutto, New natural amino acid-bearing prodrugs boost pterostilbene's oral pharmacokinetic and distribution profile, Eur. J. Pharm. Biopharm. 115 (2017) 149–158.
[38] S. Gomez-Zorita, A. Fernandez-Quintela, L. Aguirre, M.T. Macarulla, A.M. Rimando, M.P. Portillo, Pterostilbene improves glycaemic control in rats fed an obesogenic diet: involvement of skeletal muscle and liver, Food Funct. 6 (2015) 1968–1976.
[39] E. Bhakkiyalakshmi, D. Sireesh, M. Sakthivadivel, S. Sivasubramanian, P. Gunasekaran, K.M. Ramkumar, Anti-hyperlipidemic and anti-peroxidative role of pterostilbene via Nrf2 signaling in experimental diabetes, Eur. J.

Pharmacol. 777 (2016) 9–16.
[40] E. Bhakkiyalakshmi, D. Sireesh, P. Rajaguru, R. Paulmurugan, K.M. Ramkumar, The emerging role of redox-sensitive Nrf2-Keap1 pathway in diabetes, Pharmacol. Res. 91 (2015) 104–114.
[41] C.L. Hsu, Y.J. Lin, C.T. Ho, G.C. Yen, Inhibitory effects of garcinol and pterostilbene on cell proliferation and adipogenesis in 3T3-L1 cells, Food Funct. 3 (2012) 49–57.
[42] C.L. Hsu, Y.J. Lin, C.T. Ho, G.C. Yen, The inhibitory effect of pterostilbene on inflammatory responses during the interaction of 3T3-L1 adipocytes and RAW 264.7 macrophages, J. Agric. Food Chem. 61 (2013) 602–610.
[43] M.M. Hussain, Intestinal lipid absorption and lipoprotein formation, Curr. Opin. Lipidol. 25 (2014) 200–206.
[44] G. Olivecrona, Role of lipoprotein lipase in lipid metabolism, Curr. Opin. Lipidol. 27 (2016) 233–241.
[45] S. Han, T. Quach, L. Hu, A. Wahab, W.N. Charman, V.J. Stella, N.L. Trevaskis, J.S. Simpson, C.J. Porter, Targeted delivery of a model immunomodulator to the lymphatic system: comparison of alkyl ester versus triglyceride mimetic lipid prodrug strategies, J. Control Release 177 (2014) 1–10.
[46] S. Han, L. Hu, T. Quach, J.S. Simpson, N.L. Trevaskis, C.J. Porter, Profiling the role of deacylation-reacylation in the lymphatic transport of a triglyceride-mimetic prodrug, Pharm. Res. 32 (2015) 1830–1844.
[47] L. Hu, T. Quach, S. Han, S.F. Lim, P. Yadav, D. Senyschyn, N.L. Trevaskis, J.S. Simpson, C.J. Porter, Glyceride-mimetic prodrugs incorporating self-immolative spacers promote lymphatic transport, avoid first-pass metabolism, and enhance oral bioavailability, Angew. Chem. Int. Ed. Engl. 55 (2016) 13700–13705.
[48] S. Han, L. Hu, Gracia, T. Quach, J.S. Simpson, G.A. Edwards, N.L. Trevaskis, C.J. Porter, Lymphatic transport and lymphocyte targeting of a triglyceride mimetic prodrug is enhanced in a large animal model: studies in greyhound dogs, Mol. Pharm. 13 (2016) 3351–3361.
[49] A. Mattarei, M. Azzolini, M. La Spina, M. Zoratti, C. Paradisi, L. Biasutto, Amino acid carbamates as prodrugs of resveratrol, Sci. Rep. 5 (2015) 15216.
[50] M. Azzolini, A. Mattarei, M. La Spina, E. Marotta, M. Zoratti, C. Paradisi, L. Biasutto, Synthesis and evaluation as prodrugs of hydrophilic carbamate ester analogues of resveratrol, Mol. Pharm. 12 (2015) 3441–3454.
[51] A. Mattarei, M. Azzolini, M. Carraro, N. Sassi, M. Zoratti, C. Paradisi, L. Biasutto, Acetal derivatives as prodrugs of resveratrol, Mol. Pharm. 10 (2013) 2781–2792.
[52] D.C. Forbes, D.G. Ene, M.P. Doyle, Stereoselective synthesis of substituted 5-hydroxy-1,3-dioxanes, Synthesis 1998 (1998) 879–882.